Acta Histochemica 125 (2023) 152001

Contents lists available at ScienceDirect

Acta Histochemica

journal homepage: www.elsevier.com/locate/acthis

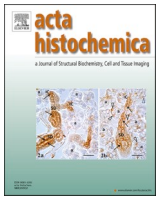

Calsequestrin in Purkinje cells of mammalian cerebellum

Sandra Furlan [a], Beatrice Paradiso [b], Elisa Greotti [a,c,d], Pompeo Volpe [c], Alessandra Nori [c,*,1]

[a] National Research Council, Institute of Neuroscience, 35121 Padova, Italy
[b] General Pathology Unit, Dolo Hospital, Riviera XXIX Aprile, 2, 30031 Dolo, Venice, Italy
[c] University of Padova, Department of Biomedical Sciences and Interdepartmental Research Center of Myology (cirMYO), 35131 Padova, Italy
[d] Padova Neuroscience Center (PNC), University of Padova, Padua, Italy

ARTICLE INFO

Keywords:
Ca Stores
Calsequestrin
Purkinje cells
Cerebellum

ABSTRACT

Cerebellum is devoted to motor coordination and cognitive functions. Endoplasmic reticulum is the largest intracellular calcium store involved in all neuronal functions. Intralumenal calcium binding proteins play a pivotal role in calcium storage and contribute to both calcium release and uptake. Calsequestrin, a key calcium binding protein of sarco-endoplasmic reticulum in skeletal and cardiac muscles, was identified in chicken and fish cerebellum Purkinje cells, but its expression in mammals and human counterpart has not been studied in depth. Aim of the present paper was to investigate expression and localization of Calsequestrin in mammalian cerebellum. Calsequestrin was found to be expressed at low level in cerebellum, but specifically concentrated in Calbindin D28- and zebrin- immunopositive-Purkinje cells. Two additional fundamental calcium store markers, sarco-endoplasmic calcium pump isoform 2, SERCA2, and Inositol-trisphosphate receptor isoform 1, IP3R1, were found to be co-expressed in the region, with some localization peculiarities. In conclusion, a new marker was identified for Purkinje cells in adult mammals, including humans. Such a marker might help in staminal neuronal cells specification and in dissection of still unknown neurodegeneration and physio-pathological effects of dys-regulated calcium homeostasis.

1. Introduction

1.1. Endoplasmic reticulum in regulation of neuronal function

In neurons, endoplasmic reticulum (ER) is involved in pre-synaptic vesicle release, neuronal activity dependent gene expression, post-synaptic (dendritic spines) plasticity, mitochondrial bioenergetics, morphogenesis of axodendritic compartment and control of development. All these different functions are made possible by ER structural and molecular heterogeneity. ER membrane surface area is much larger than plasma membrane surface since is made up by tightly packed interconnected sheets in cell body and dendrites and by narrow tubular structures in axons (Terasaki et al., 2013; Volpe et al., 1993). Dendritic spines contain a specialized ER structure, the spine apparatus i.e., stacks of smooth ER alternated to electron dense material (dense internal plaques). Multiple stimuli induce calcium (Ca^{2+}) release from ER through IP3R1 and RYR channels via two main mechanisms: Ca^{2+} induced Ca^{2+}release (CICR) and IP3R-Induced Ca^{2+}release. Both channels are activated and inhibited by different Ca^{2+}concentrations and the two mechanisms are often coordinated.

1.2. Calcium stores

Regulation of Ca^{2+} homeostasis is the key mechanism in neuronal functions and its alterations are involved in many human pathological conditions (Brini et al., 2014). ER compartments (membrane and lumen) are enriched in Ca^{2+} release channels, Ca^{2+} pumps and resident Ca^{2+} binding proteins. Three isoforms of both Ryanodine sensitive channels (RYR1, RYR2, RYR3, Abu-Omar et al., 2018) and Inositol trisphosphate sensitive channels (IP3R1, IP3R2, IP3R3, Hisatsune and Mikoshiba, 2017) are expressed in mouse brain, RYR1 and IP3R1 being preferentially expressed in cerebellum Purkinje cells (PC). In the lumen of

Abbreviations: Casq, calsequestrin mouse gene; CASQ, calsequestrin human gene; Casq, mouse/human calsequestrin protein; CBL, cerebellum; CBR, mouse total brain without cerebellum; ER, endoplasmic reticulum; GCL, granule cell layer; IP3R1, Inositol-trisphosphate receptor isoform 1 mouse/human protein; ML, molecular layer; PC, Purkinje Cell; RYR, Ryanodine Receptor Ca^{2+} channel; SERCA2, sarco-endoplasmic reticulum calcium pump isoform 2.

* Correspondence to: Department of Biomedical Sciences, via Ugo Bassi 58/B, 35131 Padova, Italy.
E-mail address: alessandra.nori@unipd.it (A. Nori).
[1] ORCID 0000-0003-3968-9450.

https://doi.org/10.1016/j.acthis.2023.152001
Received 1 June 2022; Received in revised form 11 January 2023; Accepted 16 January 2023
Available online 18 January 2023

neuronal ER, calreticulin is the ubiquitously expressed Ca^{2+} binding protein whereas very little is known about other specific intra ER Ca^{2+} binding proteins in mammalian neurons.

1.3. Calsequestrin (Casq) in brain

Low affinity high capacity Ca^{2+} binding proteins allow accumulation and storage of releasable Ca^{2} necessary to sustain Ca^{2+} release and uptake. Casq is the principal intralumenal Ca^{2+} binding protein of skeletal and cardiac muscle Sarcoplasmic Reticulum; it forms complexes with RYR and Casq-specific anchor proteins (junctin and triadin). There are two genes encoding two Casq isoforms (Arai et al., 1992): the cardiac (Casq2) isoform is expressed in heart myocytes and slow-twitch skeletal muscle fibers, whereas the skeletal (Casq1) isoform is expressed in both fast- and slow-twitch skeletal muscle fibers. In boars, Casq is expressed in total protein homogenates of the hippocampus (Weaver et al., 2000; Ambrogini et al., 2020) and, at low level, of hypothalamus and frontal cortex (Weaver et al., 2000). Little is known about the neuron specific molecular organization of IP3R1 and RYR channels with ER Ca^{2+} binding proteins in mammalian cerebellum (Nori et al., 1993). Extensive studies have been performed in chicken cerebellum in the nineties of last century. By immunogold labeling and immunofluorescence, Casq was identified in vesicles with dense core belonging to smooth ER, co-enriched in either IP3R or RYR. These structures were described in cell body of PC, dendrites and axons but excluded from spines (Takei et al., 1992; Villa et al., 1991; Volpe et al., 1990, 1991, 1993). Other studies showed that both chicken and rat ER compartments of PC dendritic spines were enriched in IP3R but devoid of RYR (Ellisman et al., 1990; Walton et al., 1991).

Recently we identified two Casq isoforms in *Danio rerio* (zebrafish) brain and cerebellum: Casq1 was expressed in granular cell layer of cerebellum and in optic tectum, a characteristic cerebellum-like structure of non-mammalian vertebrates equivalent to the superior colliculus, whereas Casq2 concentrated in PC at cell bodies, axons, proximal and distal dendritic shafts (Furlan et al., 2020).

The aim of the present paper is to identify Casq in adult mouse and human cerebellum and to study its cellular expression in relation to principal ER Ca^{2+}-store associated proteins.

2. Materials and methods

2.1. Tissue sources

Experiments were carried out on three brains for mRNA and protein analysis and three brains for immunofluorescence analysis of adult (3 months old) male C57 mice. Experimental protocols have been approved by University of Padua Review Boards protocol number D2784.N.PDJ.

Human brain tissues were obtained from two autopsies (referred to as 56 and 136). The autopsy samples were obtained from two women (whose ages were 64 and 70 years old) with no recorded neurological alterations. The sampling procedure was approved by the Institutional Ethical Committee. Specimens were routinely fixed in 10 % neutral buffered formalin, sectioned axially in half, processed, and then embedded in paraffin. The paraffin block was sectioned at 10 μm. Slides were manually stained for hematoxylin/eosin and immunofluorescence analysis. A part of the specimen was otherwise deep-frozen in liquid nitrogen for mRNA and protein analysis. A sample of skeletal muscle biopsy was used for total mRNA and protein extraction.

2.2. Protein extraction methods and analysis

Cerebral cortex, cerebellum and skeletal muscle protein extracts were prepared as follow. Tissues were grounded in liquid nitrogen, then homogenized with a Teflon pestle equipped Potter-Elvehjem Tissue grinder in the presence of a medium containing 3 % (wt/vol) SDS, 0.1 mM EGTA, pH 7.0, 0.2 mM PMSF (penylmethanesulphonyl fluoride), 1 μM leupeptin and 0.8 mM benzamidine. Homogenates were then boiled for 5 min and clarified at 15,000 *g* for 10 min. Supernatants were used as whole protein extracts. Protein concentration was determined by the method of Lowry using bovine serum albumin as a standard. Protein samples were separated by electrophoresis on 10 % SDS polyacrylamide gels and transferred to nitrocellulose filter membrane. The membranes were blocked in Tris-Buffered Saline Tween-20 (TBST) containing 5 % skimmed milk powder for 1 h then incubated with the polyclonal rabbit anti-calsequestrin antibody (Thermo Fisher Scientific PA1-913, diluted 1:1000 in TBST), or monoclonal mouse anti-calsequestrin antibody (Thermo Fisher Scientific MA3-913, diluted 1:1000 in TBST) at 4 °C for 14–16 h. After extensive washing, the membranes were incubated with a 1:5000 dilution of Anti-Rabbit IgG–Alkaline Phosphatase antibody (Sigma-Aldrich A3687) or Anti-Mouse IgG–Alkaline Phosphatase antibody (Sigma Aldrich A9316) one hour at room temperature. Specific protein bands were detected by premixed BCIP®/NBT solution (Sigma B6404).

2.3. RNA extraction and PCR-qPCR analysis

Total RNA was obtained from mouse brain cerebral cortex, cerebellum and skeletal muscles, and human specimen of skeletal muscle and cerebellum, using TRIzol® extraction method. Reverse transcription and qPCR were carried out as previously described (Furlan et al., 2020). Primers sequence was designed with the Primer3 software (Whitehead Institute for Biomedical Research, Cambridge, MA, USA; http://frodo.wi.mit.edu/), and their thermodynamic specificity was determined using BLAST sequence alignments [U.S. National Center for Biotechnology Information (NCBI), Bethesda, MD, USA] and Vector NTI® (Invitrogen) Software.↱ For qPCR analysis, all samples were run simultaneously with RNA- and RT-negative controls. Normalization was performed by ΔCT method using B2M, PPIA or Polr2f for mouse and B2M or GAPDH for human samples respectively. Same data trends were obtained with all reference genes for each species. Values are expressed as mean (n = 3) ± SEM.

Primers sequences were as follows:

m_Casq1	Fw	CAGACAAGCCCAACAGTGAA
	Rv	CAGGCTTCAGTTTCCTCAGG
m_Casq2	Fw	TCAAAGACCCACCCTACGTC
	Rv	GTCACTCTTCTCCGCAAAGG
m_B2M	Fw	GGAAGCCGAACATACTGAACTG
	Rv	TCCCGTTCTTCAGCATTTGG
m_PPIA	Fw	AGCATGTGGTCTTTGGGAAGGTG
	Rv	CTTCTTGCTGGTCTTGCCATTCC
m_Polr2f	Fw	CGACGACTTTGATGACGTTG
	Rv	GCTCACCAGATGGGAGAATC
h_casq2	Fw	TTGCCATCCCCAACAAACCT
	Rv	ACGAGCAGAGGAAAGTCGTC
h_B2M	Fw	TATCCAGCGTACTCCAAAGA
	Rv	GACAAGTCTGAATGCTCCAC
h_GAPDH	fw	CACCATCTTCCAGGAGCGAG
	Rv	TTCACACCCATGACGAACAT

For endpoint PCR, on human samples, cDNA from different tissues were amplified under standard conditions using the same h_casq2 primer pair as in qPCR, and amplicons were analyzed in 2 % agarose gel. The PCR product was 268 bp long.

2.4. Immunofluorescence

After sacrifice, mouse brains were quickly removed, briefly washed in cold phosphate buffered saline PBS, fixed overnight in 4% paraformaldehyde diluted in PBS, dehydrated through graded ethanol and embedded in paraffin as previously described (Furlan et al., 2020). Immunofluorescence analysis was performed on 8 μm thick serial parasagittal sections. Sections were deparaffinized and rehydrated in graduated ethanol, then heated for 20 min in boiling Sodium citrate buffer (10 mM Sodium citrate, 0.05 % Tween 20, pH 6.0) for antigen

retrieval, before permeabilization with a 0,1 % Triton in PBS for 20 min. Sections were then treated with blocking buffer M.O.M.® (Mouse on Mouse) Blocking Reagent (Vector Laboratories, Inc., CA, United States) 1:50 in PBST for 1 h to avoid non-specific staining and then incubated with specific antibodies (see Table 1 supplementary material for dilutions) in PBS, 1 % Goat Serum, 0.1 % Tween-20 for 120 min at room temperature. The specificity of anti-IP3R1 was previously described in rat CBL (Nori et al., 1993). Sections were rinsed in PBS, incubated for 60 min at room temperature with, goat anti-Mouse IgG (H + L) Secondary Antibody, Alexa Fluor™ 488, A-11001, goat anti-Mouse IgG (H + L) Secondary Antibody Alexa Fluor™ 594, A-11005, goat anti-Rabbit IgG (H + L) Secondary Antibody, Alexa Fluor™ 594, A-11012, 1:300 dilution, Thermo Fisher Scientific, rinsed again in PBS and mounted with ProLong Gold antifade reagent with DAPI (Thermo Fisher Scientific Life Sciences) and coverslip. Images were taken on a Leica DMR Epifluorescence microscope, a Leica TCS SP5 confocal microscope, a Leica TCS SP5 II confocal microscope equipped with Leica HyD hybrid detector, a ZEISS Elyra 7 with Lattice SIM super-resolution microscope.

Epi-fluorescence analysis (Figs. 2, 3) was carried out by a Leica DMR microscope equipped with an HBO 50 W lamp and CCD Microscope Camera Leica DFC365 FX; NPlan 10X/0.25 (Fig. 2 supplementary material) or HCX PL FLUOTAR 40X/0.75 (Figs. 2, 3) dry objectives were used. Filter systems; Leica L5 for blue excitation, excitation filter: BP 480/40, dichromatic mirror: 505, suppression filter 527/30; Leica Filter N2.1 for green excitation, excitation filter: BP 515–560, dichromatic mirror: 580, suppression filter: LP 590. Digitized images were acquired by Leica Application Suite Advanced Fluorescence 4.0.0.11706 (LASAF) Software.

Confocal analysis single immunofluorescent staining (Fig. 5 panels A–D, Fig. 7 panels C, -E). Images were collected by a Leica TCS SP5 II confocal microscope using a WLL white laser (Leica) equipped with a PlanApo 100 × (numerical aperture 1.4) oil immersion objective equipped with Leica HyD hybrid detector. The detector gain and the laser power was adjusted and maintained among different experiments to minimize background and avoid saturation. For all images, the pinhole was set to 1 Airy unit. Confocal microscopy imaging was performed at 1024 × 1024 pixels per image, with a 200 Hz acquisition rate. Zoom and scanning steps have been adjusted according to the Nyquist sampling. Digitized images were acquired by using Leica Application Suite Advanced Fluorescence 4.0.0.11706 (LASAF) Software.

Confocal analysis double immunofluorescent staining (Fig. 4) images were collected by using a Leica TCS SP5 confocal microscope with lambda blue 63.0x/1.40 NA oil-immersion objective. The lasers were: excitation wavelength 488 nm power 36 % for Casq and 15 % for IP3R1 and collection of emitted light optimized in the 500–535 nm range (green) and an excitation wavelength 561 nm laser power 29 % for SERCA, collection of emitted light was optimized in the 607–662 nm range (red). Images were 1.024 × 1.024 pixels the scanning was in sequential mode, scan speed 200 Hz. Digitized images were acquired by using Leica Application Suite Advanced Fluorescence 4.0.0.11706 (LASAF) Software.

Super-resolution analysis single immunofluorescent staining (Fig. 5 Panels E-H). Images were collected by using a ZEISS Elyra 7 with Lattice SIM with Plan-Apochromat 63x/1.4 Oil DIC M27 objective, at a wavelength of 488 nm; images were 2560 × 2560 pixels, scan speed 200 Hz.

Software for image elaboration: images were digitally processed with Adobe Photoshop or ImageJ software.

2.5. Histochemistry

The haematoxylin and eosin (H&E) images were automatically acquired by Leica DMRA2 microscope equipped with 10x/0.30. N Plan objective.

2.6. Antibodies

Primary antibodies: Anti-Calsequestrin Thermo Fisher Scientific (catalog number PA1-913) rabbit polyclonal; Anti-Calsequestrin Thermo Fisher Scientific (catalog number MA3-913) mouse monoclonal; Anti-CalbindinD28 Synaptic System (catalog number 214011) mouse monoclonal; Anti-IP3R1 custom made (Nori et al., 1993) rabbit

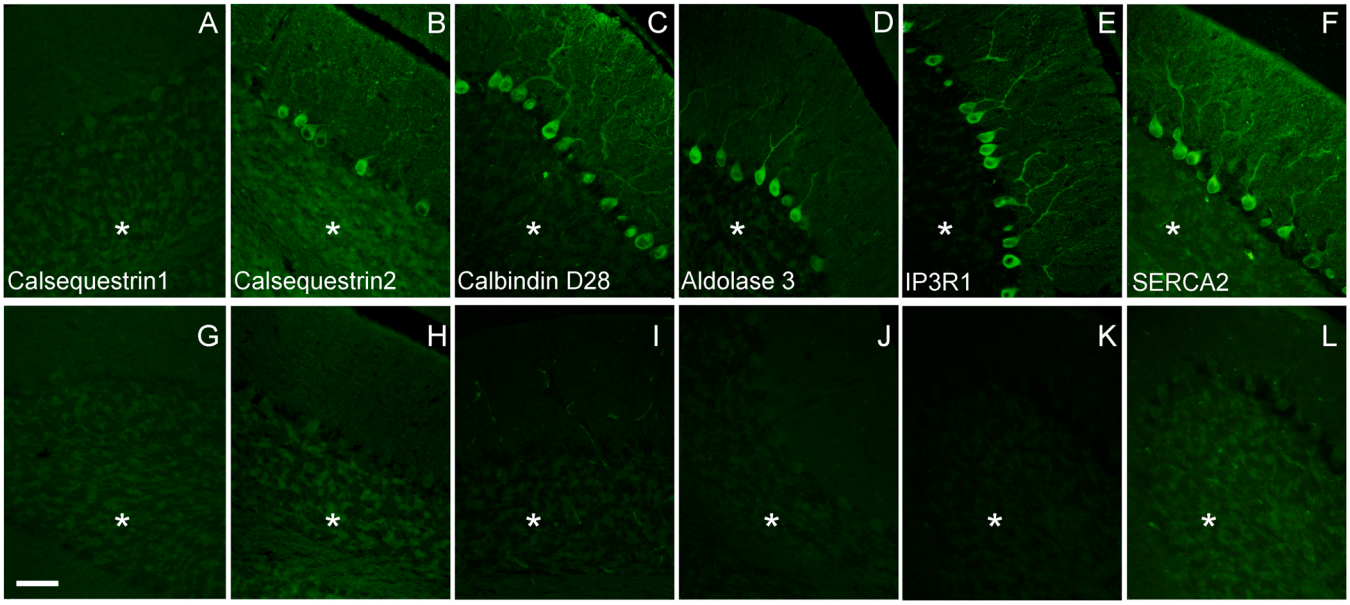

Fig. 2. Background analysis for antibodies used in the immunofluorescence staining study. Epifluorescence signal obtained by anti-Casq1 MA3-913 and Goat anti-Mouse Alexa Fluor™ 488 (A), anti Casq2 PA1-913 and Goat anti-Rabbit Alexa Fluor™ 488 (B), anti-Calbindin D28 and Goat anti-Mouse Alexa Fluor™ 488 (C), anti-Aldolase 3 and Goat anti-Rabbit Alexa Fluor™ 488 (D), anti-IP3R1 and Goat anti-Rabbit Alexa Fluor™ 488 (E), anti-SERCA2 and Goat anti-Mouse Alexa Fluor™ 488 (F) antibodies in adult mouse CBL. Background controls performed omitting primary antibody are shown in G–L respectively. Images were obtained with identical microscope settings between A and G, B and H, C and I, D and J, E and K, F and L. All stainings were performed on sagittal, paraffine embedded 8 μm sections. Asterisks indicate the GCL. Scale bar: 50 μm.

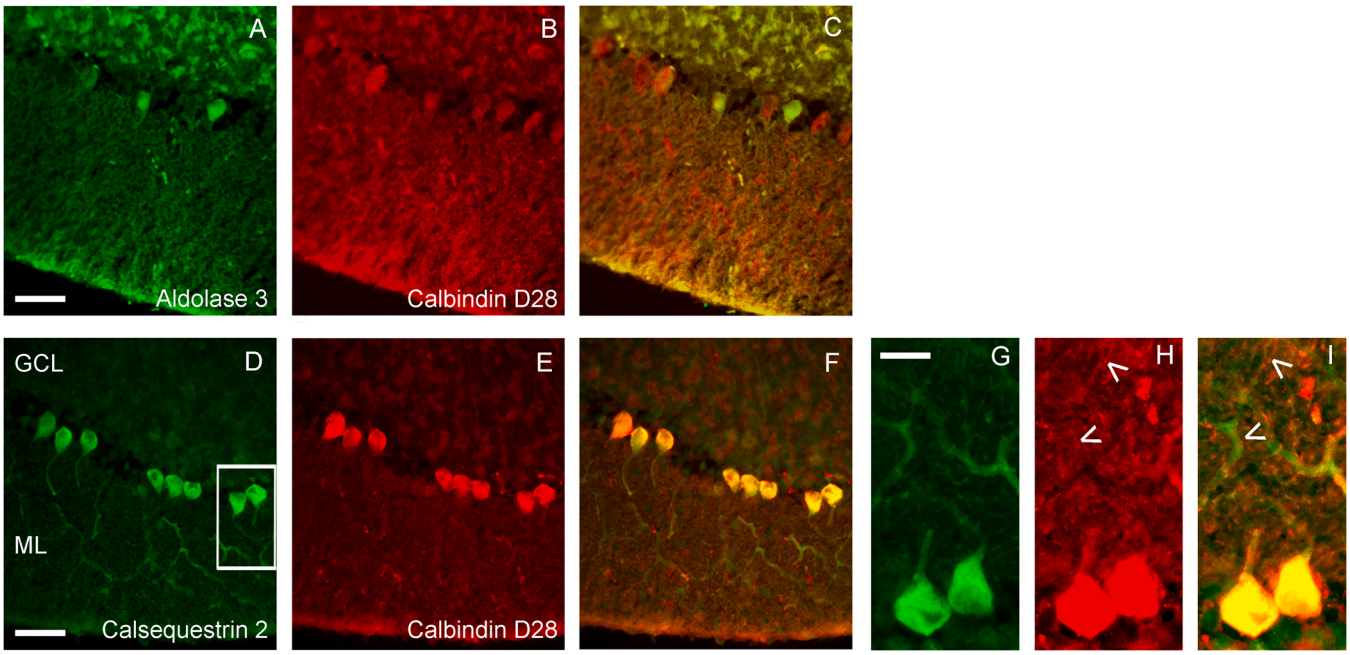

Fig. 3. Double immunofluorescent staining for Casq2, Calbindin D28, Aldolase 3 in mouse CBL. (A-F) Representative epifluorescence signal obtained by anti-Calbindin D28 and Goat anti-Mouse Alexa Fluor™ 594 (B, E), anti-Aldolase 3 and Goat anti-Rabbit Alexa Fluor™ 488 (A) and anti-Casq PA1-913 and Goat anti-Rabbit Alexa Fluor™ 488 (D) antibodies. Panels C, F, I show the merged view of left and middle panels of the same row. Note in panel B eight PC immunopositive for Calbindin D28 and in panel A three of them which show different Aldolase 3 content. (G–I) Higher-magnification views of the double immunofluorescent staining shown in D–F. Magnified areas are indicated by box in D. In panels G–I image brightness and contrast were adjusted to visualize structures immunopositive for Calbindin D28 and negative for Casq2 (arrowheads). Panels A–F present same orientation of granular cell layer (GCL) upward, and molecular layer (ML) downward. Scale bar: A–F 50 μm; G–I 20 μm.

polyclonal; Anti-SERCA2, Abcam (catalog number AB2861) mouse monoclonal; Anti-Aldolase3 Abcam (catalog number AB87122) rabbit polyclonal.

Secondary antibodies: Goat anti-Mouse IgG (H + L) Cross-Adsorbed Secondary Antibody, Alexa Fluor™ 488; Goat anti-Mouse IgG (H + L) Cross-Adsorbed Secondary Antibody, Alexa Fluor™ 594; Goat anti-Rabbit IgG (H + L) Cross-Adsorbed Secondary Antibody, Alexa Fluor™ 488; Goat anti-Rabbit IgG (H + L) Cross-Adsorbed Secondary Antibody, Alexa Fluor™ 594 Thermo Fisher Scientific. For further information on antibodies see Table 1 in Supplementary material.

3. Results

3.1. Mouse cerebellum expresses calsequestrin2 mRNA and protein

Mouse cerebellum (CBL) was separated from cerebrum (CBR) and total mRNA was extracted from both organs and analyzed Fig. 1. Fig. 1A shows the comparative expression of Casq1 and Casq2 mRNA in CBL and CBR. Messenger RNA of *Casq2* is enriched in CBL whereas *Casq1* mRNA is barely detected. Slow-twitch Soleus muscle was investigated as positive control for *Casq1* and *Casq2* mRNAs. Expression of Casq2 was investigated by western blot with a commercial polyclonal antibody raised against cardiac Casq2 which preferentially recognizes Casq2, and, with very low affinity, mouse Casq1. As shown in Fig. 1 B, a 55 kDa protein band corresponding to Casq2 is detectable in Soleus muscle protein extract and in CBL, albeit at lower intensity. Antibody specificity for mouse brain Casq was previously shown by Ambrogini et al. (2020)., who compared by western blot wild-type and double Casq1–2 null homogenates obtained from hippocampus. Casq1, on the contrary, is detectable in fast twitch-skeletal muscle as a 63 kDa band that is absent in both CBR and CBL; this finding was confirmed by means of Casq1-specific antibodies which detect no signal in CBL (Fig. 1 supplementary material).

3.2. Casq2 is enriched in Purkinje cells of mouse cerebellum

Cellular localization of Casq2 and other known cytoplasmic Ca^{2+} binding proteins, Calbindin D28 and Aldolase 3, was studied by immunofluorescence of CBL sagittal sections at the vermis level. Background signal for all antibodies used in the present study was analyzed comparing the signal obtained in immunofluorescence experiment (Fig. 2 upper panels) with the signal obtained omitting the primary antibody (Fig. 2 lower panels). As shown in Fig. 2, panel A, Casq1 signal is not different from control (panel G). Conversely, Casq2, Calbindin D28 and Aldolase 3 are concentered in PC cell bodies and dendrites (panels B, C, D). Both Calbindin D28 and Aldolase 3 are known PC markers (Celio, 1990; Dlugos, 2015; Lee et al., 2010; Schwaller et al., 2002) with different specificity; in fact, Calbindin D28 is described as a general marker of PC whereas Aldolase 3 immunopositive PC are organized in transversal stripes alternated to negative stripes (Hawkes and Herrup, 1995), panel 3 represents a positive zone. Immunofluorescence analysis of whole CBL sagittal sections at vermis level was performed for Casq2, Calbindin D28 and Aldolase 3 to compare their overall cell expression (Fig. 2 supplementary material). Casq2 and Calbindin D28-immunopositive cells were detectable in all lobules, whereas Aldolase 3 (zebrin) was detectable in PC of specific zones, as expected. Fluorescence signal of anti-IP3R1 and anti-SERCA2 antibodies and respective background is shown in panels E, K and F, L respectively (see next section for details).

Identification of PC cells expressing Casq2 was further accomplished by double immunofluorescent staining. As shown in Fig. 3 panels A–C, PC expressing both Aldolase 3 and Calbindin D28 were recognizable even if with different relative signal intensity (see legend to Fig. 3 for further details). Double immunofluorescent staining with anti-Casq and anti-Calbindin D28 (Fig. 3 panels D–F) shows homogeneous co-expression of the two proteins in PC cell bodies. At higher magnification, Calbindin D28-immunopositive puncta are identifiable in dendritic branches (white arrowheads in Fig. 3, panels H, I), according to what is

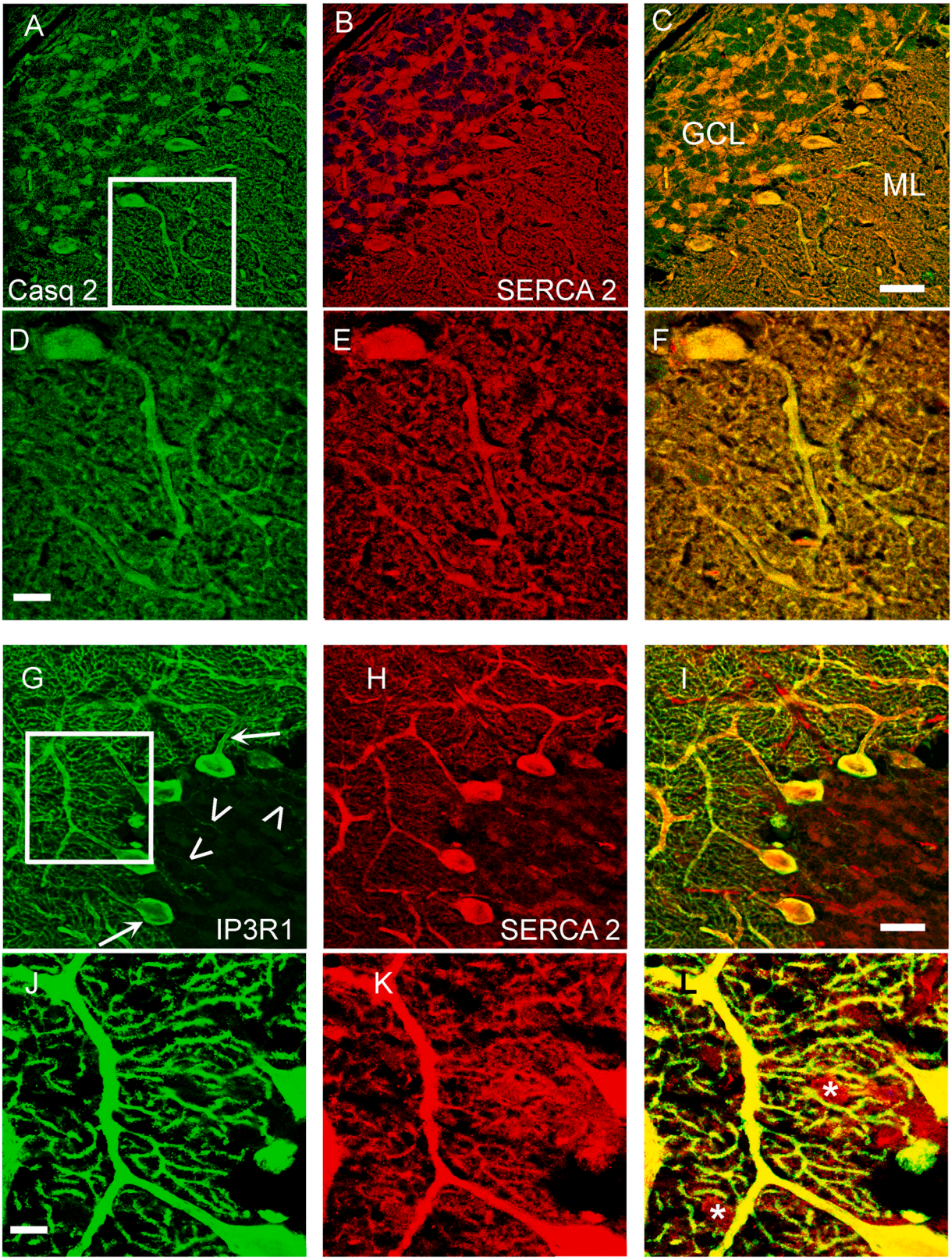

Fig. 4. Confocal analysis of double immunofluorescent staining for Casq2, SERCA2 calcium pump and IP3R1 calcium channel in mouse CBL. Representative images obtained by anti-Casq PA1-913 and Goat anti-Rabbit Alexa Fluor™ 488 (A), anti-SERCA2 and Goat anti-Mouse Alexa Fluor™ 594 (B, H) and anti-IP3R1 and Goat anti-Rabbit Alexa Fluor™ 488 (G) antibodies. Sequence of channel acquisition was blue, red, green with same Z position in sequential mode, frame average was 4 for all channels and both experiments. Each panel on the right is a merged view of the left and middle panels of the same row, scale bar 25 μm. Higher-magnification and increased brightness images of the double immunofluorescent staining are shown in panels D–F and J–L, magnified areas are indicated by boxes in A and G. Pixel size 240,5 nm panels A–C and G–I; 80,1 nm panels D–F and J–L. Arrowheads in panel G indicate PC axons immunopositive for IP3R1; arrows in panel G indicate accumulation of IP3R1 signal in periphery of cell body and primary dendrites; asterisks in panel L indicate cells immunopositive for SERCA2 and negative for IP3R1 signal in the molecular layer. A–C and G–I present same orientation of ML and GCL. Scale bar: 10 μm.

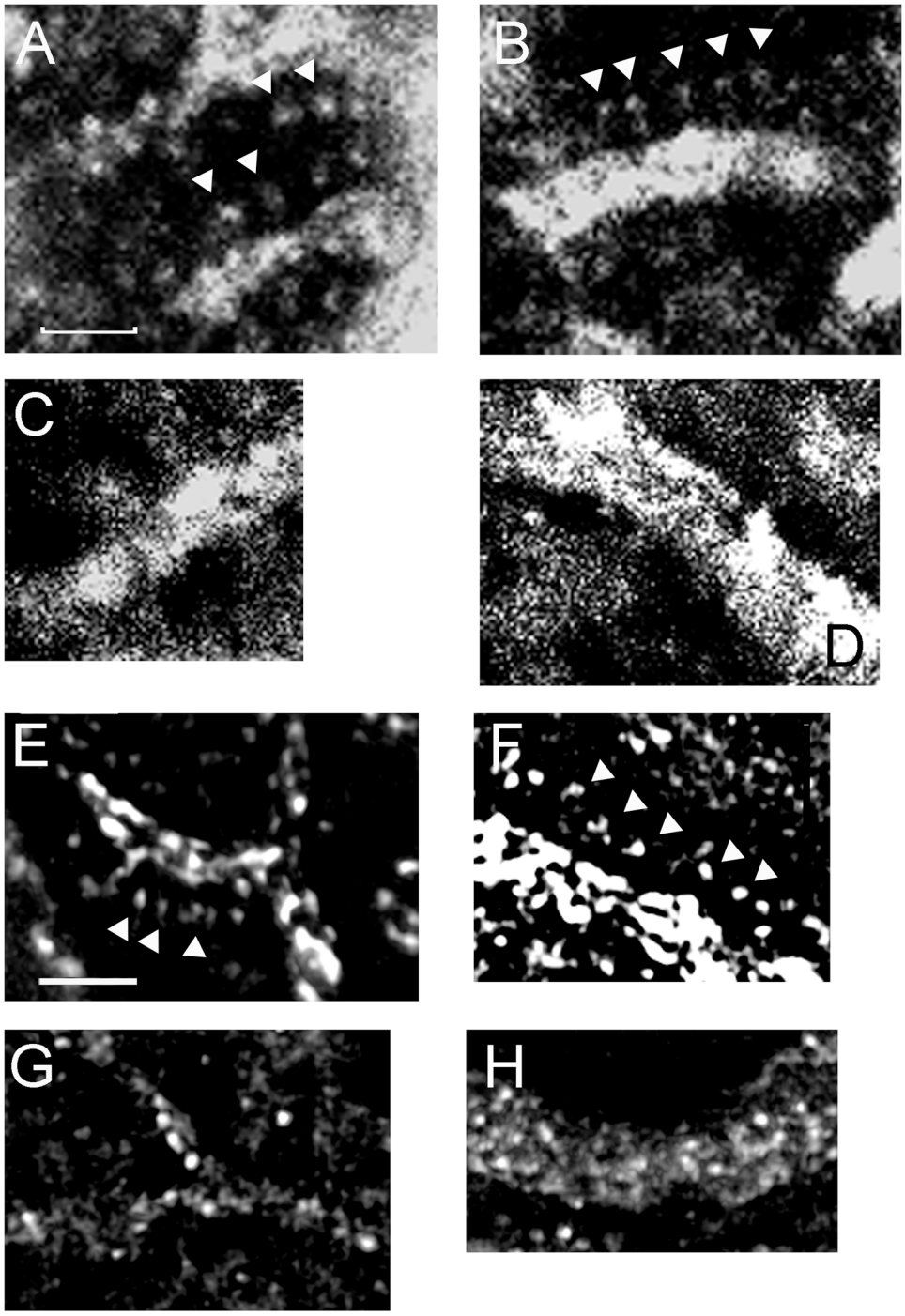

Fig. 5. Dendritic branches decorated by anti-IP3R1 (panels A, B, E, F) or anti-Casq antibodies (panels C, D, G, H) were analyzed by two different systems (TCS SP5 II confocal microscope panels A-D, and Elyra 7 super-resolution microscope panels E-H, see methods for details). A variable number of optical section images in the z-dimension was collected, the maximal intensity projection is shown. Spines emerging from both proximal and distal dendrites are shown in panels A, B, E, F (arrowheads indicate some spines immunopositive for IP3R1). Note that few spines appear directly connected to the dendrite. Pixel size: panels A–D x 46 nm, y 46 nm, z 138 nm; panels E–H pixel size 32,24 nm. Bar 2 μm. In Fig. 3 supplementary material the complete images are shown.

described in rat (Dlugos, 2015), whereas a corresponding condensed signal for Casq2 is lacking. Moreover, pearl-like structures with condensed Casq2 signal seem devoid of specific Calbindin D28 signal (not shown).

3.3. Co-expression of Casq2 with other calcium store markers

It is well known that IP3R and SERCA2, markers of calcium stores, are both expressed in mouse PC. Double immunofluorescent staining by anti-Casq2 and anti-SERCA2 antibodies is shown in Fig. 4, panels A–C. Casq2 immunopositive PC cell bodies and dendrites are shown. The same PC bodies and dendrites are decorated by anti-SERCA2 antibodies (panel B) with homogeneous signal distribution. Overlays of the green and red channels (merge of panels C and F) show that the signals co-localize with homogeneous distribution at cell bodies and dendrites. In the molecular layer, primary and peripheral dendritic branchlets show co-presence of the two signals in C and F. Fig. 4 panels G–L are representative of double immunofluorescent staining performed by anti-IP3R1 and anti-SERCA2 antibodies. As shown in panel G, IP3R1 staining is strong in PC soma and clearly decorates dendrites and axons (arrowheads), signal distribution is not homogeneous, and appears more concentrated in the periphery of both PC soma and primary large dendrites (arrows), whereas SERCA2 signal (panel H) is more homogeneously distributed. The different arrangement of IP3R1 and SERCA2 signals is clear in merge panel I in which the red color (SERCA2 signal, red channel) is preferentially located in the center of PC bodies and

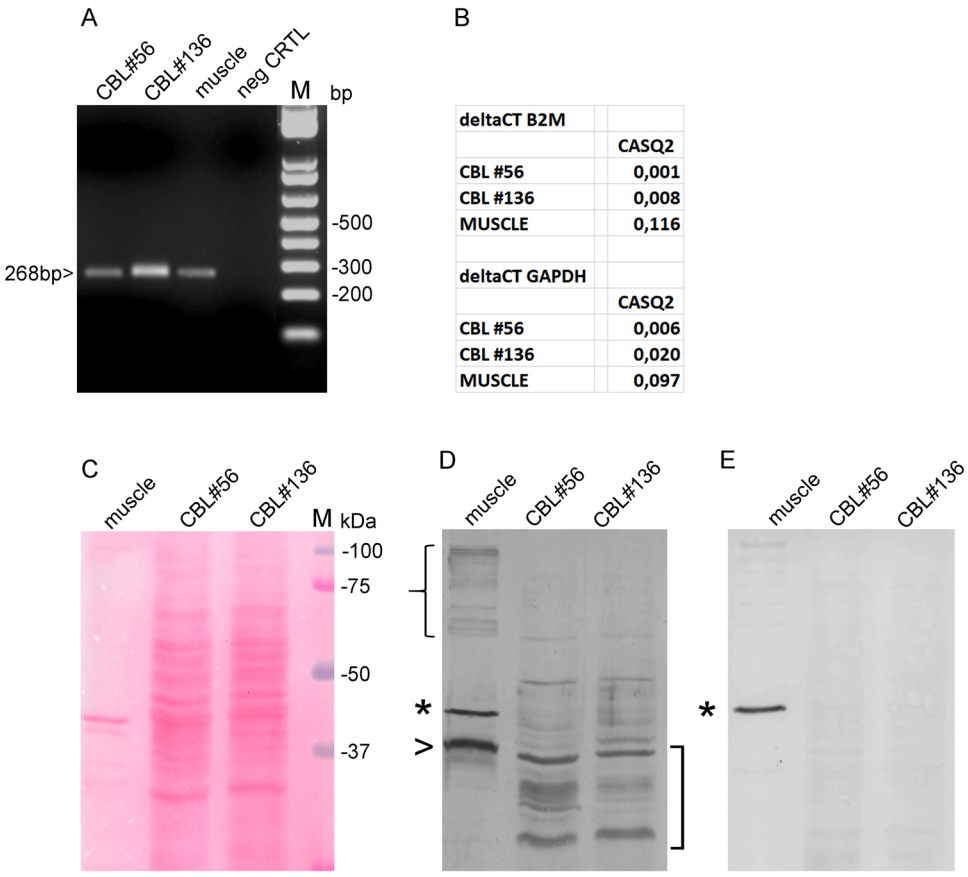

deltaCT B2M	
	CASQ2
CBL #56	0,001
CBL #136	0,008
MUSCLE	0,116
deltaCT GAPDH	
	CASQ2
CBL #56	0,006
CBL #136	0,020
MUSCLE	0,097

Fig. 6. Casq2 expression in human CBL. (A) Agarose gel showing PCR products of *CASQ2* gene obtained from two human CBL extracts (subject 56 and 136) and skeletal muscle. 4 ng of PCR product from CBL and 0.8 ng from skeletal muscle (positive control) were loaded per well. Negative control (CRTL) was performed omitting the cDNA. 1 kb ladder was used as marker (M); bp base pair. (B). *Casq2* m RNA expression in the indicated tissues are normalized to B2M and GAPDH housekeeping genes. Mean relative expressions were determined from triplicate runs of the qPCR assay. (C) Total protein ponceau red staining, 50 μg of CBL and 5 μg of muscle homogenates, were loaded. (D, E) immunoblot analysis with anti-Casq showing immunoreactive pattern in human muscle, 56 and 136 CBL homogenates. Human muscle tissue extract was used as positive control. (D) anti-cardiac Casq PA1-913 antibody (E) anti-skeletal Casq MA3-913 antibody. Immunoreactive bands at 60k Casq1 (asterisk) and 50k Casq2 (arrowhead). Square bracket indicates protein smear. Calsequestrin-like proteins in human muscle homogenate are indicated with a curly bracket. Molecular weight markers are shown. kDa kilodalton.

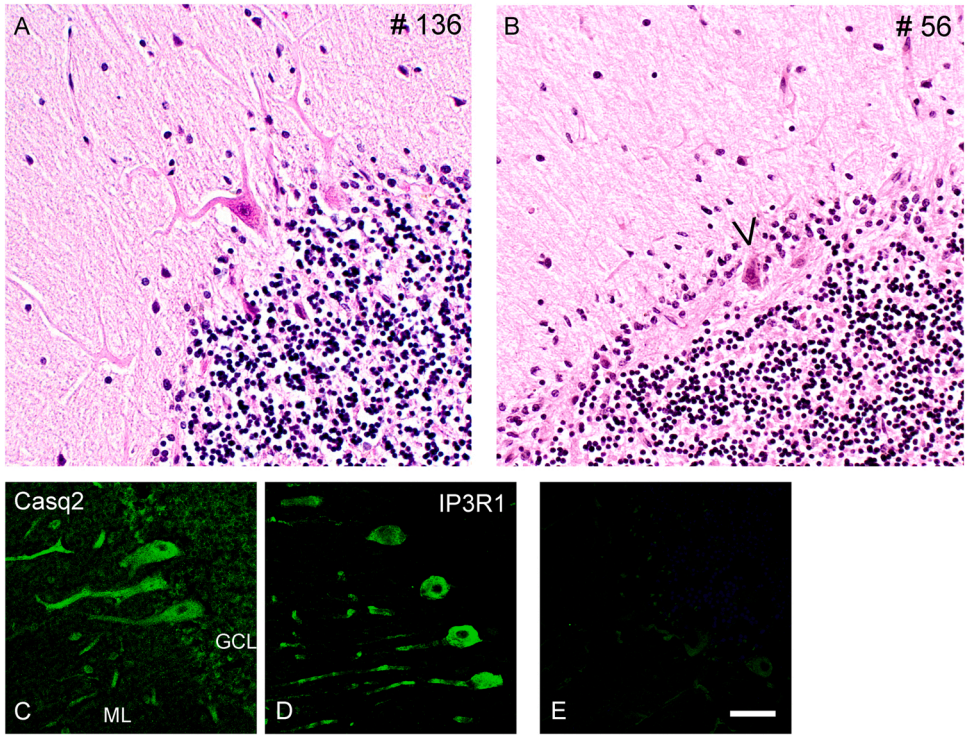

Fig. 7. Immunofluorescence analysis of Casq2 and IP3R1 expression in human CBL. Hematoxylin and eosin staining of sagittal sections from the biopsy of subject 136 (A) and 56 (B) were performed on paraffine-embedded sections (10 μm). Arrowhead indicates a degenerated PC. (C) Confocal single immunofluorescence signal of subject 136 obtained by anti-Casq2 antibody (PA1-913) and Goat anti-Rabbit Alexa Fluor™ 488 in a CBL section. (D) Confocal single immunofluorescence signal obtained by anti-IP3R1 antibody and Goat anti-Rabbit Alexa Fluor™ 488 in a CBL section. (E) Background signal obtained by secondary anti-rabbit Alexa Fluor®488 with acquisition settings identical to panel C. Scale bar: 50 μm.

dendrites, whereas the yellow color indicating co-localization of red and green channels is more peripherally located. The peripheral concentration of IP3R1 is compatible with its expression at subplasmalemmal cisternal elements of PC described in rat CBL by colloidal gold labeling and confocal microscopy (Nori et al., 1993; Sandonà et al., 2003; Takei et al., 1992) as well as in other neurons (Wu et al., 2017).

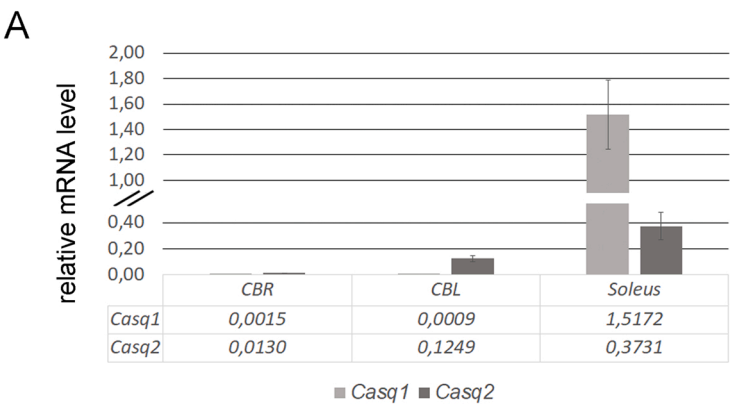

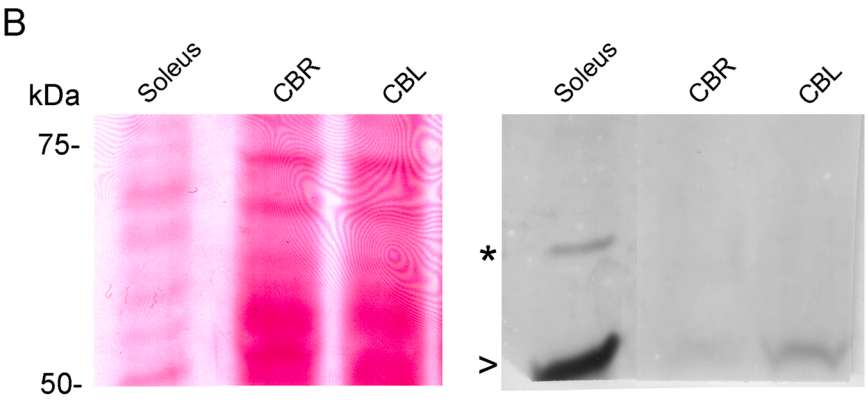

Fig. 1. Casq2 expression in adult mouse brain tissues. (A) Quantitative PCR-analysis of *Casq1* and *Casq2* mRNAs in CBR, CBL and muscle from adult mice. *Casq* mRNA relative expressions in the indicated tissues are normalized to B2M housekeeping gene, same trends were observed if PPIA or Polr2f were used as reference genes (not shown). Mean values (n = 3) and standard error were determined from triplicate runs of the qPCR assay in three different tissue preparations. (B) Casq2 protein expression in tissue homogenates. Left panel, ponceau staining of total protein: 50 μg of protein extract from CBR and CBL and 20 μg from Soleus muscle. Right panel, the same blot after testing for Casq using specific antibodies (PA1-913). Arrowhead: Casq 2; asterisk: Casq1. Molecular weight markers are shown on the left. kDa kilodalton.

At higher magnification spiny branches are identifiable by anti-IP3R1 antibodies (Fig. 4 panels J, L) suggesting the widespread distribution of IP3R1 into the spine compartment. Anti-SERCA2 antibodies do not decorate all IP3R1-immunopositive structures; moreover, some cells of the molecular external and internal molecular layers, are labeled with anti-SERCA2 antibodies and lack the IP3R1 signal (two of them are indicated by asterisks in Fig. 4 panel L). Higher resolution images of the PC spine compartment were obtained at two additional microscopes (Fig. 5), dendritic fragments surrounded with spines from different areas of the molecular layer are shown. In Panels A, B, IP3R1 immunopositive dendritic spines are resolved by confocal high-sensitivity low-noise microscopy (see methods for details). Dendritic branches appear decorated by aligned spines identifiable by dense positive puncta located at about 0.8–1 μm distance from dendrites, reasonably representing IP3R1 expressed at spine head ER. On the contrary, rows of fluorescent puncta along PC dendrites are not observed by anti-Casq2 antibody (see panels C, D). The different compartmentalization of IP3R1 and Casq2 was further addressed and analyzed by a super-resolution microscope (see methods for details). Examples of IP3R1 positive structures aligned along dendritic branches with a pattern almost identical to panels A, B are shown in panels E, F. The Casq2 signal is better resolved under these experimental conditions, yet immune-positive structures aligned along dendrites were not observed. Representative images are shown in panels G, H.

3.4. *Casq2 is expressed in PC of human cerebellar cortex*

In total human brain *CASQ2* mRNA is expressed at low level in comparison with skeletal and cardiac muscles (Human Protein Atlas proteinatlas.org; Sjöstedt et al., 2020); moreover, data on protein expression are not available. The present findings in mouse PC suggest that Casq2 should be identifiable in human CBL. For this reason, two human cerebella at vermis level were analyzed for *CASQ2* mRNA and protein expression. Low level of *CASQ2* mRNA is detectable by qPCR (Fig. 6B). This observation is confirmed by end point PCR which produces a 268 bp fragment both in human CBL and skeletal muscle, the latter being a tissue where *CASQ2* is largely expressed (panel A). Total protein homogenates were obtained from both human cerebellar cortexes and analyzed by western blot in order to identify Casq2. A faint band having a molecular weight compatible with that of muscle Casq2 is detectable (Fig. 6 panel D, arrowheads), in addition to a protein smear probably indicating immunoreactive peptides from Casq2 degradation (square bracket). Anti-Casq1 specific antibodies do not show any signal in both CBL samples (panel E). Moreover, high molecular weight bands (curly bracket) are visible in muscle homogenate and, at lower intensity, in cerebellum. In muscle these proteins have been previously reported as calsequestrin-like proteins (Knollmann et al., 2006). Small number of PC and partial protein degradation in cerebellum total homogenate could be responsible for the low signal obtained in western blot. In order to identify cells expressing Casq2, both human cerebella cortexes were sectioned at vermis level and stained with haematoxylin and eosin (H&E) or decorated with anti-IP3R1 and anti-Casq2 antibodies (Fig. 7). H&E staining of the cortex of both samples (Fig. 7, panels A, B) shows a different degree of preservation of PC structure clearly visible at the level of soma; in particular sample 56 shows highly pyknotic nuclei, shrinkage of cytoplasm and loss of dendritic tree indicating PC degeneration (arrowheads), on the contrary, sample 136 displays a more normal PC structure. Both quantitative mRNA analysis (Fig. 6 panel B) and immunoblot (Fig. 6 panel D) show higher Casq2 signal in sample 136 than in sample 56; for these reasons sample 136 was chosen for experiments pertaining to Casq2 cellular localization (Fig. 7 panels C–E). Panels C and D, shows two cerebellar serial sections decorated by either anti-Casq2 or anti-IP3R1 antibodies, respectively. PC bodies and dendrites expressing both Casq2 and IP3R1 are clearly identifiable.

4. Discussion

4.1. Mouse cerebellum Purkinje cells express Casq2

In this paper, we identify Casq2 as a component of cerebellum Ca^{2+} stores and validate it as a PC marker following the suggestion based on the microarray study by Rong et al. (2004). According to transcriptomic and proteomic analyses performed on total mouse CBL (Corradini et al., 2014; Fecher et al., 2019; Lein et al., 2007; Pavlidis and Noble, 2001) and PC (Rong et al., 2004), we found that Casq2 is enriched in mouse CBL at mRNA and protein levels as previously shown in other animal species, i.e. birds and fishes (Volpe et al., 1993; Furlan et al., 2020). The present data show that Casq1 mRNA is identifiable in trace amounts (Fig. 1 panel A). Casq1 protein is not detectable at protein level as shown in western blot and immunofluorescence obtained by anti Casq1-specific antibody (Fig. 1 supplementary material and Fig. 2 panel A), Casq1 RNA traces, detected in total CBL mRNA, likely belong to vascular smooth-muscle cells that express both Casq isoforms (Volpe et al., 1994). In conclusion, Casq1 does not seem to be expressed in neuronal cells of mammalian CBL, at variance with fishes where both *casq1a and casq1b* mRNA were measured and the corresponding proteins were also expressed (Furlan et al., 2020).

Here we show enrichment of Casq2 in PC cell body, a finding in accordance with the high ER volume of these cells (Karagas and Venkatachalam, 2019). The cell-type peculiar expression of Casq2 is different from that of Calreticulin, an ER Ca^{2+} binding chaperone protein, that is diffuse in all CBL neurones (Cassidy et al., 2013) and from that of Parvalbumin a stellate, basket and PC cytoplasmic Ca^{2+} buffer (Schwaller et al., 2002). Biophysical properties of Casq are different from those of Calreticulin. Casq is a low affinity Ca^{2+} binding protein undergoing Ca^{2+} dependent polymerization and de-polymerization with Ca^{2+} capacity increase in the polymerized form and confers the dynamic strong buffering capacity of Sarcoplasmic Reticulum terminal cisternae (Manno et al., 2017). Moreover, as to localization, Casq polymers are anchored to precise Sarcoplasmic Reticulum compartments (terminal cisternae) by two specific anchor proteins (junctin and triadin) in the proximity of Ca^{2+} release channels (Rossi et al., 2021). It is interesting to note that mRNA of Junctin, has been identified in total brain (Hong et al., 2001) and is highly expressed in mouse PC (Allen Mouse Brain Atlas [71380950], 2011 https://mouse.brain-map.org/experiment/show/71380950). Such Casq characteristics are suitable to confer structural specificity as well as dynamic functional buffering properties to ER Ca^{2+} stores in mammalian PC.

4.2. Co-expression of Casq2 with other Ca^{2+} store markers

Known Ca^{2+} store markers such as SERCA2 and IP3R1 are expressed in mammalian cerebellum (Mata and Sepúlveda, 2005; Sepulveda et al., 2004; Kakizawa et al., 2020; Cassidy et al., 2013). In the present paper Casq2 is shown to be localized in cell body and primary dendritic arbor as SERCA2, but seems to be absent from protruding spines which are identified by anti IP3R1 antibody. The characteristic spotty punctuate fluorescence pattern obtained by anti-Casq2 antibodies is detectable both in primary and secondary dendrites suggesting concentration of Casq2 in discrete ER compartments. It remains to be ascertained the nature of such structures. In chicken PC Casq enrichment has not been observed in ER of spines, but often at their base (Villa et al., 1991): limited optical resolution and the lack of a generic structural marker of spines do not allow a clear cut explanation for this observation; on the other hand, Casq2-immunopositive compartments might be stubby spines which do not protrude from the dendrite like mushroom or thin spines and account for 15 % of PC total spines (Lee et al., 2005). Additional studies are needed in order to explore this issue. In conclusion, the present paper provides the first evidence of a Casq2 expressing compartment in mammalian PC. Further studies are needed to unveil its precise sub-cellular localization and to characterize the related sub-cellular compartment, although both puncta and diffuse Casq2 labeling observed in mouse PC are indeed similar to that observed in chicken PC. In skeletal and cardiac muscles, it is well established that Casq is a Sarcoplasmic Reticulum dynamic Ca^{2+} buffer involved in Ca^{2+} transient shaping and Ryanodine receptor Ca^{2+} channel (RYR) modulation; consequently, it is plausible that Casq plays such functional roles in neuronal Ca^{2+} signaling too.

4.3. Perspectives on Casq2 expression in Purkinje cells

Such studies will give the opportunity to look at PC Ca^{2+} homeostasis from a different point of view, i.e., from inside the ER store both in physiological and pathological conditions. Moreover, experimentation on knock-out (CASQ2-/-), (Denegri et al., 2012; Knollmann, 2006; Valle et al., 2016) and knock-in (R33Q/R33Q) (Rizzi et al., 2008; Valle et al., 2020) models for Casq2 would provide additional, crucial information. The role of Casq2 in neuronal function and synaptic plasticity can be postulated considering the function of intraluminal Ca^{2+} binding proteins in the modulation of Ca^{2+} transients and their implication in synaptic plasticity. In chicken Purkinje cells cytoplasmic Ca^{2+} transients have been measured upon activation of both glutamate and metabotropic receptors indicating Ca^{2+} release from either IP3-sensitive or ryanodine- sensitive Ca^{2+} stores (Sacchetto et al., 1995). As to mammalian Purkinje cells, it has been demonstrated by Finch and Augustine (1998) that prolonged stimulation of the cerebellum parallel fibers activates Ca^{2+} release from the endoplasmic reticulum of dendrites locally, as well as from individual dendritic spines, via IP3R; the same authors explore the role of IP3 in the long-term depression (LTD) of parallel fiber synapses and demonstrate that IP3-stimulated Ca^{2+} release was sustained throughout the period of stimulation and that sustained and large Ca^{2+} release is an essential feature of LTD. Here the role of Casq2 could come into play: by increasing the Ca^{2+} store capacity, Casq2 would allow the LTD response in the synapses between parallel fibers and Purkinje cells. A second paper by Gomez et al. (2020) addresses Ca^{2+} release via IP3R in different axonal compartments and shows that the Ca^{2+} signal appears to be restricted to defined areas and does not expand to neighboring areas. Such Ca^{2+} signals originating from intracellular Ca^{2+} stores in PCs may be explained on the basis of the high cytoplasmic Ca^{2+} buffering due to the presence of large concentrations of parvalbumin and calbindin. Under these conditions, filling of the Ca^{2+} stores by SERCA could be slowed down and a strong intraluminal dynamic buffer, due to Casq2, might be necessary for a lasting and repeatable response over time.

To the best of our knowledge, this is the first report on Casq2 expression in PC of adult humans. The present findings pave the way to more precise dissection of many human pathological conditions. Evidence is accruing as to derangement of IP3R-dependent Ca^{2+} signaling in many neurological diseases, such as Alzheimer (Miguel et al., 2021) and Parkinson diseases, spinocerebellar ataxia, Huntington disease, epilepsy, autism, Gillespie syndrome (Berridge, 2016; Hisatsune and Mikoshiba, 2017), Amyotrophic Lateral Sclerosis (Staats et al., 2016), as well as in the pathogenesis of long-term depression of memory (Inoue et al., 1998). Enrichment of *CASQ2* mRNA in human thalamus (Human Protein Atlas proteinatlas.org; Sjöstedt et al., 2020) suggests a hypothetical involvement of Casq2 in cerebellum-thalamic-cortical circuitry. The discovery of Casq2, a strong dynamic buffer, in human PC cells could also contribute to understanding pathogenetic mechanisms which involve release of Ca^{2+} from ER.

CRediT authorship contribution statement

Sandra Furlan: Conceptualization, Methodology, Investigation, Visualization, Writing – review & editing. **Beatrice Paradiso:** Methodology, Resources, Writing – review & editing. **Elisa Greotti:** Methodology Investigation, Visualization. **Pompeo Volpe:** Resources, Writing – review & editing, Funding acquisition. **Alessandra Nori:**

Conceptualization, Methodology, Investigation, Writing – original draft, Writing – review & editing, Funding acquisition.

All authors have read and approved the final manuscript.

Conflict of interest

The authors have no conflicts of interest to declare.

Data Availability

Data will be made available on request.

Acknowledgements

Human cerebella samples were provided by Cristina Basso, Department of Cardiac, Thoracic and Vascular Sciences and Public Health, University of Padua. We thank Roberta Sacchetto Department of Comparative Biomedicine and Food Science University of Padova, Italy for technical support and critically reading the manuscript. Gabriele Baj and Agnes Thalhammer Centro Interdipartimentale di Microscopia Avanzata "Carlo e Dirce Callerio" -**CIMA** Università degli Studi di Trieste for super-resolution analysis for technical support in super-resolution analysis. This work was supported by funds from the University of Padova, Progetti di Ateneo BIRD201323/20 and DOR2099545/20 to AN.

Appendix A. Supporting information

Supplementary data associated with this article can be found in the online version at doi:10.1016/j.acthis.2023.152001.

References

Abu-Omar, N., Das, J., Szeto, V., Feng, Z.-P., 2018. Neuronal ryanodine receptors in development and aging. Mol. Neurobiol. 55 (2), 1183–1192. https://doi.org/10.1007/s12035-016-0375-4.

Allen Mouse Brain Atlas [71380950], 2011. Available from mouse.brain-map.org. Allen Institute for Brain Science.

Ambrogini, P., Lattanzi, D., di Palma, M., Ciacci, C., Savelli, D., Galati, C., Gioacchini, A. M., Pietrangelo, L., Vallorani, L., Protasi, F., Cuppini, R., 2020. Calsequestrin deletion facilitates hippocampal synaptic plasticity and spatial learning in post-natal development. Int. J. Mol. Sci. 21 (15), 5473. https://doi.org/10.3390/ijms21155473.

Arai, M., Otsu, K., MacLennan, D.H., Periasamy, M., 1992. Regulation of sarcoplasmic reticulum gene expression during cardiac and skeletal muscle development. Am. J. Physiol.-Cell Physiol. 262 (3), C614–C620. https://doi.org/10.1152/ajpcell.1992.262.3.C614.

Berridge, M.J., 2016. The inositol trisphosphate/calcium signaling pathway in health and disease. Physiol. Rev. 96 (4), 1261–1296. https://doi.org/10.1152/physrev.00006.2016.

Brini, M., Calì, T., Ottolini, D., Carafoli, E., 2014. Neuronal calcium signaling: function and dysfunction. Cell. Mol. Life Sci. 71 (15), 2787–2814. https://doi.org/10.1007/s00018-013-1550-7.

Cassidy, L.L., Dlugos, F.F., Dlugos, C.A., 2013. Time course of SERCA 2b and calreticulin expression in purkinje neurons of ethanol-fed rats with behavioral correlates. Alcohol Alcohol. 48 (6), 667–678. https://doi.org/10.1093/alcalc/agt062.

Celio, M.R., 1990. Calbindin D-28k and parvalbumin in the rat nervous system. Neuroscience 35 (2), 375–475. https://doi.org/10.1016/0306-4522(90)90091-H.

Corradini, E., Vallur, R., Raaijmakers, L.M., Feil, S., Feil, R., Heck, A.J.R., Scholten, A., 2014. Alterations in the cerebellar (phospho)proteome of a cyclic guanosine monophosphate (cGMP)-dependent protein kinase knockout mouse. Mol. Cell. Proteom. 13 (8), 2004–2016. https://doi.org/10.1074/mcp.M113.035154.

Denegri, M., Avelino-Cruz, J.E., Boncompagni, S., de Simone, S.A., Auricchio, A., Villani, L., Volpe, P., Protasi, F., Napolitano, C., Priori, S.G., 2012. Viral gene transfer rescues arrhythmogenic phenotype and ultrastructural abnormalities in adult calsequestrin-null mice with inherited arrhythmias. Circ. Res. 110 (5), 663–668. https://doi.org/10.1161/CIRCRESAHA.111.263939.

Dlugos, C.A., 2015. Ethanol-induced alterations in purkinje neuron dendrites in adult and aging rats: a review. Cerebellum 14 (4), 466–473. https://doi.org/10.1007/s12311-014-0636-6.

Ellisman, M.H., Deerinck, T.J., Ouyang, Y., Beck, C.F., Tanksley, S.J., Walton, P.D., Airey, J.A., Sutko, J.L., 1990. Identification and localization of ryanodine binding proteins in the avian central nervous system. Neuron 5 (2), 135–146. https://doi.org/10.1016/0896-6273(90)90304-X.

Fecher, C., Trovò, L., Müller, S.A., Snaidero, N., Wettmarshausen, J., Heink, S., Ortiz, O., Wagner, I., Kühn, R., Hartmann, J., Karl, R.M., Konnerth, A., Korn, T., Wurst, W., Merkler, D., Lichtenthaler, S.F., Perocchi, F., Misgeld, T., 2019. Cell-type-specific profiling of brain mitochondria reveals functional and molecular diversity. Nat. Neurosci. 22 (10), 1731–1742. https://doi.org/10.1038/s41593-019-0479-z.

Finch, E.A., Augustine, G.J., 1998. Local calcium signaling by inositol-1,4,5-trisphosphate in Purkinje cell dendrites. Nature 396, 753–756. https://doi.org/10.1038/25541.

Furlan, S., Campione, M., Murgia, M., Mosole, S., Argenton, F., Volpe, P., Nori, A., 2020. Calsequestrins new calcium store markers of adult zebrafish cerebellum and optic tectum. Front. Neuroanat. *14*. https://doi.org/10.3389/fnana.2020.00015.

Gomez, L.C., Kawaguchi, S., Collin, T., Llano, I., 2020. Influence of spatially segregated IP3-producing pathways on spike generation and transmitter release in Purkinje cell axons. Proc. Natl. Acad. Sci. USA 117, 11097–11108. https://doi.org/10.1073/pnas.2000148117.

Hawkes, R., Herrup, K., 1995. Aldolase C/zebrin II and the regionalization of the cerebellum. J. Mol. Neurosci. 6 (3), 147–158. https://doi.org/10.1007/BF02736761.

Hisatsune, C., Mikoshiba, K., 2017. IP3 receptor mutations and brain diseases in human and rodents. J. Neurochem. 141 (6), 790–807. https://doi.org/10.1111/jnc.13991.

Hong, C.S., Kwak, Y.G., Ji, J.H., Chae, S.W., Han Kim, D., 2001. Molecular cloning and characterization of mouse cardiac junctate isoforms. Biochem. Biophys. Res. Commun. 289 (4), 882–887. https://doi.org/10.1006/BBRC.2001.6056.

Inoue, T., Kato, K., Kohda, K., Mikoshiba, K., 1998. Type 1 inositol 1,4,5-trisphosphate receptor is required for induction of long-term depression in cerebellar Purkinje neurons. J. Neurosci. 18 (14), 5366–5373. https://doi.org/10.1523/JNEUROSCI.18-14-05366.1998.

Kakizawa, S., Kishimoto, Y., Yamamoto, S., Onga, K., Yasuda, K., Miyamoto, Y., Watanabe, M., Sakai, R., Mori, N., 2020. Functional maintenance of calcium store by ShcB adaptor protein in cerebellar Purkinje cells. Sci. Rep. 10 (1), 14475. https://doi.org/10.1038/s41598-020-71414-y.

Karagas, N.E., Venkatachalam, K., 2019. Roles for the endoplasmic reticulum in regulation of neuronal calcium homeostasis. Cells 8 (10), 1232. https://doi.org/10.3390/cells8101232.

Knollmann, B.C., 2006. Casq2 deletion causes sarcoplasmic reticulum volume increase, premature Ca^{2+} release, and catecholaminergic polymorphic ventricular tachycardia. J. Clin. Investig. https://doi.org/10.1172/JCI29128.

Lee, J.C., Chung, Y.H., Cho, Y.J., Kim, J., Kim, N., Cha, C.I., Joo, K.M., 2010. Immunohistochemical study on the expression of calcium binding proteins (calbindin-D28k, calretinin, and parvalbumin) in the cerebellum of the nNOS knock-out(-/-) mice. Anat. Cell Biol. 43 (1), 64. https://doi.org/10.5115/acb.2010.43.1.64.

Lee, K.J., Kim, H., Rhyu, I.J., 2005. The roles of dendritic spine shapes in Purkinje cells. Cerebellum 4 (2), 97–104. https://doi.org/10.1080/14734220510007842.

Lein, E.S., Hawrylycz, M.J., Ao, N., Ayres, M., Bensinger, A., Bernard, A., Boe, A.F., Boguski, M.S., Brockway, K.S., Byrnes, E.J., Chen, L., Chen, L., Chen, T.-M., Chi Chin, M., Chong, J., Crook, B.E., Czaplinska, A., Dang, C.N., Datta, S., Jones, A.R., et al., 2007. Genome-wide atlas of gene expression in the adult mouse brain. Nature 445 (7124), 168–176. https://doi.org/10.1038/nature05453.

Manno, C., Figueroa, L.C., Gillespie, D., Fitts, R., Kang, C., Franzini-Armstrong, C., Rios, E., 2017. Calsequestrin depolymerizes when calcium is depleted in the sarcoplasmic reticulum of working muscle. Proc. Natl. Acad. Sci. USA 114 (4). https://doi.org/10.1073/pnas.1620265114.

Mata, A.M., Sepúlveda, M.R., 2005. Calcium pumps in the central nervous system. Brain Res. Rev. 49 (2), 398–405. https://doi.org/10.1016/j.brainresrev.2004.11.004.

Miguel, J.C., Perez, S.E., Malek-Ahmadi, M., Mufson, E.J., 2021. Cerebellar calcium-binding protein and neurotrophin receptor defects in down syndrome and Alzheimer's disease. Front. Aging Neurosci. *13*. https://doi.org/10.3389/fnagi.2021.645334.

Nori, A., Villa, A., Podini, P., Witcher, D.R., Volpe, P., 1993. Intracellular Ca^{2+} stores of rat cerebellum: heterogeneity within and distinction from endoplasmic reticulum. Biochem. J. 291 (1), 199–204. https://doi.org/10.1042/bj2910199.

Pavlidis, P., Noble, W.S., 2001. Analysis of strain and regional variation in gene expression in mouse brain. Genome Biol. 2 (10), research0042.1 https://doi.org/10.1186/gb-2001-2-10-research0042.

Rizzi, N., Liu, N., Napolitano, C., Nori, A., Turcato, F., Colombi, B., Bicciato, S., Arcelli, D., Spedito, A., Scelsi, M., Villani, L., Esposito, G., Boncompagni, S., Protasi, F., Volpe, P., Priori, S.G., 2008. Unexpected structural and functional consequences of the R33Q homozygous mutation in cardiac calsequestrin. Circ. Res. 103 (3), 298–306. https://doi.org/10.1161/CIRCRESAHA.108.171660.

Rong, Y., Wang, T., Morgan, J.I., 2004. Identification of candidate Purkinje cell-specific markers by gene expression profiling in wild-type and pcd3J mice. Mol. Brain Res. 132 (2), 128–145. https://doi.org/10.1016/j.molbrainres.2004.10.015.

Rossi, D., Gamberucci, A., Pierantozzi, E., Amato, C., Migliore, L., Sorrentino, V., 2021. Calsequestrin, a key protein in striated muscle health and disease. J. Muscle Res. Cell Motil. 42 (2), 267–279. https://doi.org/10.1007/s10974-020-09583-6.

Sacchetto, R., Cliffer, K.D., Podini, P., Villa, A., Christensen, B.N., Volpe, P.1995. Intracellular Ca^{2+} stores in chick cerebellum Purkinje neurons: ontogenetic and functional studies. Am. J. Physiol., vol. 269(no. 5 Pt 1), pp. C1219–27. ⟨https://doi.org/10.1152/ajpcell.1995.269.5.C1219⟩. (PMID: 7491912).

Sandonà, D., Scolari, A., Mikoshiba, K., Volpe, P., 2003. Subcellular distribution of Homer 1b/c in relation to endoplasmic reticulum and plasma membrane proteins in Purkinje neurons. Neurochem. Res. 28 (8), 1151–1158. https://doi.org/10.1023/A:1024264025401.

Schwaller, B., Meyer, M., Schiffmann, S., 2002. "New" functions for "old" proteins: the role of the calcium-binding proteins calbindin D-28k, calretinin and parvalbumin, in cerebellar physiology. Studies with knockout mice. Cerebellum 1 (4), 241–258. https://doi.org/10.1080/147342202320883551.

Sepulveda, M.R., Hidalgo-Sanchez, M., Mata, A.M., 2004. Localization of endoplasmic reticulum and plasma membrane Ca^{2+}-ATPases in subcellular fractions and sections of pig cerebellum. Eur. J. Neurosci. 19 (3), 542–551. https://doi.org/10.1111/j.0953-816X.2003.03156.x.

Sjöstedt, E., Zhong, W., Fagerberg, L., Karlsson, M., Mitsios, N., Adori, C., Oksvold, P., Edfors, F., Limiszewska, A., Hikmet, F., Huang, J., Du, Y., Lin, L., Dong, Z., Yang, L., Liu, X., Jiang, H., Xu, X., Wang, J., Mulder, J., 2020. An atlas of the protein-coding genes in the human, pig, and mouse brain. Science 367 (6482). https://doi.org/10.1126/science.aay5947.

Staats, K.A., Humblet-Baron, S., Bento-Abreu, A., Scheveneels, W., Nikolaou, A., Deckers, K., Lemmens, R., Goris, A., van Ginderachter, J.A., van Damme, P., Hisatsune, C., Mikoshiba, K., Liston, A., Robberecht, W., van den Bosch, L., 2016. Genetic ablation of IP_3 receptor 2 increases cytokines and decreases survival of $SOD1^{G93A}$ mice. Hum. Mol. Genet. 25 (16), 3491–3499. https://doi.org/10.1093/hmg/ddw190.

Takei, K., Stukenbrok, H., Metcalf, A., Mignery, G., Sudhof, T., Volpe, P., de Camilli, P., 1992. Ca2+ stores in Purkinje neurons: endoplasmic reticulum subcompartments demonstrated by the heterogeneous distribution of the InsP3 receptor, Ca(2+)-ATPase, and calsequestrin. J. Neurosci. 12 (2), 489–505. https://doi.org/10.1523/JNEUROSCI.12-02-00489.1992.

Terasaki, M., Shemesh, T., Kasthuri, N., Klemm, R.W., Schalek, R., Hayworth, K.J., Hand, A.R., Yankova, M., Huber, G., Lichtman, J.W., Rapoport, T.A., Kozlov, M.M., 2013. Stacked endoplasmic reticulum sheets are connected by helicoidal membrane motifs. Cell 154 (2), 285–296. https://doi.org/10.1016/j.cell.2013.06.031.

Valle, G., Vergani, B., Sacchetto, R., Reggiani, C., de Rosa, E., Maccatrozzo, L., Nori, A., Villa, A., Volpe, P., 2016. Characterization of fast-twitch and slow-twitch skeletal muscles of calsequestrin 2 (CASQ2)-knock out mice: unexpected adaptive changes of fast-twitch muscles only. J. Muscle Res. Cell Motil. 37 (6), 225–233. https://doi.org/10.1007/s10974-016-9463-3.

Valle, G., Arad, M., Volpe, P., 2020. Molecular adaptation to calsequestrin 2 (CASQ2) point mutations leading to catecholaminergic polymorphic ventricular tachycardia (CPVT): comparative analysis of R33Q and D307H mutants. J. Muscle Res. Cell Motil. 41 (2–3), 251–258. https://doi.org/10.1007/s10974-020-09587-2.

Villa, A., Podini, P., Clegg, D.O., Pozzan, T., Meldolesi, J., 1991. Intracellular Ca^{2+} stores in chicken Purkinje neurons: differential distribution of the low affinity-high capacity Ca^{2+} binding protein, calsequestrin, of Ca2+ ATPase and of the ER lumenal protein, Bip. J. Cell Biol. 113 (4), 779–791. https://doi.org/10.1083/jcb.113.4.779.

Volpe, P., Alderson-Lang, B.H., Madeddu, L., Damiani, E., Collins, J.H., Margreth, A., 1990. Calsequestrin, a component of the inositol 1,4,5-trisphosphate-sensitive Ca^{2+} store of chicken cerebellum. Neuron 5 (5), 713–721. https://doi.org/10.1016/0896-6273(90)90225-5.

Volpe, P., Villa, A., Damiani, E., Sharp, A.H., Podini, P., Snyder, S.H., Meldolesi, J., 1991. Heterogeneity of microsomal Ca^{2+} stores in chicken Purkinje neurons. EMBO J. 10 (11), 3183–3189.

Volpe, P., Nori, A., Martini, A., Sacchetto, R., Villa, A., 1993. Multiple/heterogeneous Ca^{2+} stores in cerebellum purkinje neurons. Comp. Biochem. Physiol. Part A: Physiol. 105 (2), 205–211. https://doi.org/10.1016/0300-9629(93)90196-B.

Volpe, P., Martini, A., Furlan, S., Meldolesi, J., 1994. Calsequestrin is a component of smooth muscles: the skeletal- and cardiac-muscle isoforms are both present, although in highly variable amounts and ratios. Biochem. J. 301 (2), 465–469. https://doi.org/10.1042/bj3010465.

Walton, P.D., Airey, J.A., Sutko, J.L., Beck, C.F., Mignery, G.A., Südhof, T.C., Deerinck, T. J., Ellisman, M.H., 1991. Ryanodine and inositol trisphosphate receptors coexist in avian cerebellar Purkinje neurons. J. Cell Biol. 113 (5), 1145–1157. https://doi.org/10.1083/jcb.113.5.1145.

Weaver, S.A., Schaefer, A.L., Dixon, W.T., 2000. The effects of mutated skeletal ryanodine receptors on calreticulin and calsequestrin expression in the brain and pituitary gland of boars. Mol. Brain Res. 75 (1), 46–53. https://doi.org/10.1016/S0169-328X(99)00289-2.

Wu, Y., Whiteus, C., Xu, C.S., Hayworth, K.J., Weinberg, R.J., Hess, H.F., de Camilli, P., 2017. Contacts between the endoplasmic reticulum and other membranes in neurons. Proc. Natl. Acad. Sci. USA 114 (24), E4859–E4867. https://doi.org/10.1073/pnas.1701078114.